Assessing the reproducibility of quartz OSL lifetime determinations derived using isothermal decay

Julie A. Durcan

School of Geography and the Environment, University of Oxford, Oxford, UK
*Corresponding author: julie.durcan@ouce.ox.ac.uk

Highlights

Lifetime determinations made using isothermal decay measurements are tested.
Multiple-trap signal contributions can impact lifetime determinations.
Trap depth can be well constrained, but frequency factor is more variable.
Variations in the isothermal decay protocol can lead to variability in E and s.

Abstract

Signal stability is a key consideration when using luminescence dating techniques. The stability, or lifetime, of a signal is one of the factors determining the upper age constraint for luminescence dating, and it has been suggested that the signal being used for dating should have a lifetime at least ten times the age being dated in order to limit age underestimation to an upper loss of 5%. Accurate derivations of signal stability and associated kinetic parameters, such as trap depth and frequency factor, are also important parameters for constraining rock cooling histories in thermochronometric techniques. This paper aims to assess the reproducibility of lifetime determinations derived isothermal decay measurements. Variability arising from changing the isothermal decay protocol used is tested. Simulating Arrhenius plot from fixed trap depth and frequency values shows that whilst trap depth can be relatively well constrained, significant variability in the frequency factor, hence signal lifetime, should be expected. This paper also uses luminescence signals measured using different wavelengths to better understand the impact of signal from non-fast quartz OSL components in lifetime calculations. The presence of contributions from non-fast OSL components in the initial part of the OSL signal can result in the lifetime being calculated from charge contributions from multiple traps, not solely the 325°C TL peak, as has been previously assumed. This effect can be reduced however by stimulating luminescence signals with longer wavelengths to better isolate the signal from the fast component.

Keywords

Isothermal decay, lifetime, quartz, OSL components, Arrhenius plot, E, s

1. Introduction

A key consideration when using luminescence dating for chronological applications is signal stability (Spooner and Questiaux, 2000); it is important that trapped charge populations remain at the defects in the crystal lattice of a mineral over sufficiently long periods of geological time relative to the timescale of investigation (e.g. Preusser et al., 2009). It is this signal stability which is one of the factors controlling the upper age constraint for luminescence dating, and Aitken (1985) recommends that the stability, or lifetime, of the signal should be at least ten times the age being dated in order to limit age underestimation to an upper loss of 5%. In recent years, efforts to extend the dateable age range using luminescence techniques have seen the testing and application of a range of signals from multiple dosimeters. Methods have

included (but are not limited to) violet stimulated luminescence (e.g. Ankjægaard et al., 2013) and thermally-transferred optically stimulated luminescence (e.g. Wang et al., 2006) signals in quartz, post infra-red infra-red stimulated feldspar signals (e.g. Thomsen et al., 2008), and more novel approaches such as the thermoluminescence dating of biogenic calcite (e.g. Duller et al., 2009). Key to the success of techniques aiming to extend the age range is not only a high signal saturation point, but a sufficiently long lifetime of the signal being used for dating. In addition, fundamental to optically stimulated luminescence (OSL) thermochronometry techniques is the accurate derivation of thermal kinetic parameters such as lifetime, including trap depth and frequency factor, because they are used to quantitatively constrain rock cooling histories (e.g. King et al., 2016).

There are a number of approaches which can be used to empirically derive the lifetime of a luminescence signal, including pulse annealing (e.g. Li and Tso, 1997) and isothermal decay (e.g. McKeever, 1985). Li and Chen (2001) apply both methods to a quartz sample from Hong Kong, and find that both approaches provide comparable results. In a recent study, Lowick and Valla (2018) obtained lifetime estimates from isothermal decay measurements of Swiss glacial quartz samples and Risø calibration quartz, and reported intra-sample variability of up to two orders of magnitude. They were unable to conclude whether this variability was related to their measurement protocol or whether intra-sample variability is intrinsic. Similar observations have been made by Buechi et al. (2017) and Trauerstein et al. (2017). Schmidt et al. (2018) also investigated the reproducibility of lifetime measurements of the 110°C TL peak of a single quartz sample using three different measurement techniques across eight different laboratories. They found that variability between laboratories was greater than within-laboratory variability, but that results were least dispersed when isothermal decay measurements were used. Averaged across laboratories, all three methods produce trap depth results consistent within 1σ standard deviation (Schmidt et al., 2018).

Given the importance of establishing signal lifetime when dating older samples and/or when using OSL thermochronometry techniques, this study aims to investigate the variability resulting from measurement condition selections within isothermal decay protocols to better inform estimates of the associated uncertainty. These parameters include the stimulation wavelength used for OSL measurement, and the temperature and duration of elevated temperature holds used in the measurement protocol.

2. Samples, Instrumentation, and Methodology

2.1 Samples

A Malawian lake shoreline sedimentary quartz sample (MAL05-01-01) was selected for analyses, primarily on the grounds of luminescence sensitivity and favourable luminescence properties (e.g. dose recovery within ±10% uncertainties, limited IR response at room temperature, ability to recycle a laboratory dose). The sample was prepared at Royal Holloway, University of London, according to routine sample preparation procedures detailed by Thomas et al. (2009). In this study, medium aliquots (5mm in diameter) of sample (grain size range 180-250 μm) were loaded onto 9.7 mm diameter aluminium discs and used for measurement.

2.2 Instrumentation

Luminescence measurements were made at the Oxford Luminescence Dating laboratory, University of Oxford using automated Risø TL/OSL DA-15 readers. The readers were fitted with $^{90}Sr/^{90}Y$ beta sources providing dose rates of ~3.3 and ~4.0 Gy/min. Luminescence was stimulated using blue (wavelength 470 nm, stimulation power ~30 mW cm^{-2} at 90%), green, (525 nm, ~70 mW cm^{-2} at 90%) and IR (870 nm, ~90 mW cm^{-2} at 90%) LEDs, and ultraviolet luminescence signals were detected through a bialkali photo

multiplier tube fitted with 7.5 mm U340 filters. Calibration of the reader hotplates was undertaken in 2015 and 2017, and measurements of the effective stimulation power of the LEDs were made in 2014 using an energy meter.

2.3 Signal lifetime determination

Prior to measurement, aliquots were sensitised using at least ten cycles of beta irradiation and thermoluminescence measurement up to 450°C (heating rate 5°C/s) to minimise the impact of sensitivity change during measurement. An isothermal decay protocol following that of Wang et al. (2006) was used (table 1), using temperature and hold time combinations based on those of Bailey (1998a). Isothermal decay measurements were made using visible light (green and blue; table 1a) and infra-red light (table 1b). Stimulating quartz at an elevated temperature allows the signal from the fast component to be isolated and directly measured (e.g. Bailey, 1998b, Singarayer and Bailey, 2004, Jain et al., 2005, Fan et al., 2009). The same aliquots of sample were used for all measurements. To check the reproducibility of luminescence measurements, the blue/green-light protocol (table 1a) was repeated and when signals were compared, L_x/T_x values were found to be within uncertainties.

Table 1: The isothermal decay measurement protocols used in this study. Where blue/green light stimulation was used, the protocol followed that of Wang et al., 2006 (a). Where elevated temperature IR stimulation was used, a modified protocol (following Bailey, 2010) was applied.

	Isothermal Decay Protocol	
Step	a) Blue and green LEDs	b) IR LEDs
1	Beta dose (64 Gy)	Beta dose (128 Gy)
2	Pre-heat at 220°C for 10 s	Pre-heat at 220°C for 10 s
3	Pre-heat at T°C for t s (table 2)	Pre-heat at T°C for t s (table 2)
4		IR bleach at 20°C for 20 s
5		IRSL at 160°C for 200 s (L_x)
6	CW-OSL at 125°C for 100 s (L_x)	CW-OSL at 125°C for 100 s
7	Beta dose (32 Gy)	Beta dose (128 Gy)
8	Pre-heat at 200°C for 10 s	Pre-heat at 200°C for 10 s
9		IR bleach at 20°C for 20 s
10		IRSL at 160°C for 200 s (T_x)
11	CW-OSL at 125°C for 100 s (T_x)	CW-OSL at 125°C for 100 s

Table 2: Duration (t, in seconds) of the raised temperature hold times at each temperature (T) used in step 3 of the isothermal decay measurement protocol (table 1). Hold durations are based on those applied by Bailey (1998a) who used t_1, and t_{5-8}.

	Duration (t, in seconds) of the raised temperature holds.							
T (°C)	t_1	t_2	t_3	t_4	t_5	t_6	t_7	t_8
240	0	10	100	400	1000	2000	5000	8000
245	0	7	72	290	725	1450	3450	6000
250	0	5	50	200	500	1000	2500	5000
255	0	3	32	130	325	750	1650	3000
260	0	3	30	120	300	600	1000	1500
265	0	2	21	85	212	425	775	1100
270	0	2	18	70	175	350	600	800
275	0	1	12	50	125	250	400	600
280	0	1	10	40	100	200	300	450
285	0	1	6	25	62	125	200	375
290	0	1	5	18	45	90	125	250

295	0	1	4	14	35	70	115	190
300	0	1	3	10	25	50	100	150

Assuming first order kinetics, the duration that an electron can be expected to remain trapped can be mathematically described by equation 1 (e.g. Aitken, 1985; McKeever, 1985. See also Schmidt et al., 2018).

$$\tau_T = s^{-1}.e^{\frac{E}{k_B \cdot T}} \quad \text{Equation 1}$$

In equation 1, τ_T describes the lifetime (in s) of the trap. s is the frequency factor (s^{-1}), which Aitken (1985) describes as the number of escape attempts of an electron from its trap per second. E is trap depth (in eV), or the energy required to release the electron from the trap. k_B is Boltzmann's constant (equal to 8.62 x 10^{-5} eV K^{-1}) and T is temperature (in K). In this study, values of E and s have been derived empirically. Individual aliquots were stored at a range of temperatures for varying lengths of time (as described in table 2), and measurement of the OSL signal remaining following each storage allowed estimates of the lifetime of the OSL signal at each storage temperature to be made. E and s were derived from the Arrhenius plot:

$$\ln(\tau_T) = \ln(s^{-1}) + (E/k_B).(1/T) \quad \text{Equation 2}$$

Using a plot of $\ln\tau_T$ versus 1/T, E is obtained from the gradient of the linear fit to this plot, and s from the y-axis intercept (Bailey, 1998a; e.g. figure 1).

Published isothermal decay measurement protocols have typically been less extensive than those tested in this study (table 1) and are predominately made using blue light stimulation of ultra-violet OSL signals. For example, Bailey (1998a) derives empirical estimates of τ_T at 240, 250, 260, 270, 280, and 300°C, using elevated temperature holds of t_1, t_6, t_7, t_8 in table 2. Lowick and Valla (2018) use τ_Ts of 220 240, 260 and 280°C and holds similar in magnitude to t_5, t_6, t_7, t_8 in table 2. The extended combination of temperature and hold times applied in this studied, measured using blue, green and infra-red light stimulation allows an exploration of the impact of varying the isothermal decay protocol on the calculated kinetic parameters. To investigate this variability, two key elements of the protocol are varied:

i) Stimulation wavelength. Simulating quartz with infra-red light at an elevated temperature allows the signal from the fast component to be isolated (e.g. Bailey, 1998b; Singarayer and Bailey, 2004; Jain et al., 2005). Integrating the elevated temperature IR protocol of Bailey (2010) into the isothermal decay protocol used in this study (e.g. table 1b) allows the lifetime from the fast-only signal (i.e. the 325°C thermoluminescence peak) to be calculated. In contrast, continuous-wave OSL signals stimulated with blue and green light will contain contributions from various OSL components in the initial part of the signal. However, these contributions will differ because of the wavelength dependence of photo-ionisation cross-sections with stimulation wavelength (Singarayer and Bailey, 2004). Therefore, comparison of lifetimes measured from the same aliquot using different stimulation wavelengths will allow the impact of contributions from other, non-fast OSL component contributions in lifetime calculations to be explored.
ii) Elevated temperature and hold time combinations. The effect of varying these parameters in the measurement protocol will be explored changing the elevated temperature hold (step 3 in table 1), by i) varying the combinations of hold times for τ_T derivation and ii) using different τ_T intervals for E and s derivation (e.g. temperatures every 5°C, 10°C etc. over the temperature range 240-300°C).

2.4 Component fitting of the quartz OSL signals

Curve deconvolution of visible light stimulated composite-wave OSL signals was undertaken to better understand the contribution of signal from the fast and medium quartz components to the bulk luminescence signal. Assuming first order kinetics, the luminescence signal from each component can be described mathematically (Bulur, 2000) by:

$$L_{(t)} = n_0 b exp(-bt) \quad \text{Equation 3}$$

where, $L_{(t)}$ is the luminescence intensity as a function of stimulation time t (s), n_0 is the initial trapped charge population, b is the de-trapping probability, where $b = \sigma I_0$, σ is the photo ionisation cross-section (cm^2) and I_0 is the light intensity (in photons $s^{-1}.cm^{-2}$). The sum of four exponentials was fitted to each blue/green OSL signal using SigmaPlot (following the method outlined in Durcan and Duller, 2011), and the goodness of fit was assessed through the calculation of the residual between measured and modelled signals and the R^2 value. Calculation of the % contribution of each component to the total OSL signal was made using the derived trapped charge populations (e.g. Durcan and Duller, 2011).

3. Results and Discussion

3.1 The impact of varying quartz OSL component contributions on lifetime determination

The isothermal decay protocols in table 1 were applied to the same aliquots of sample using different wavelengths of stimulation light to determine whether contributions from different quartz OSL components impact lifetime determinations. Elevated temperature IR stimulation was used to isolate signal from the fast component, with the aim of calculating a lifetime from a signal originating from the fast component trap only. Due to the wavelength dependency of quartz photo-ionisation cross sections, green and blue light was used to investigate the effects of differing contributions of components in the initial part of the OSL signals on lifetime determination. Table 3 summarises E, s and τ_{20} (lifetime at ambient temperature) calculated from the same aliquots using blue, green and IR LEDs. There is a relationship between E and wavelength, with longer wavelengths providing higher trap depths and longer lifetimes. Of particular interest is i) the relatively high values of E, s, and lifetime using the elevated temperature IR protocol and ii) the discrepancy between the green and blue light stimulated E and lifetimes values. The IR-E values of 1.88 ± 0.16 and 1.99 ± 0.18 are higher than published estimates of E for the 325°C quartz TL peak, which are typically in the region of 1.65 eV (e.g. Wintle and Murray, 1998; Murray and Wintle 1999; Preusser et al.,2009; Lowick and Valla, 2018). These are associated with excessively high s values, hence high lifetimes. Investigation of the relationship between elevated temperature IR luminescence and hold time (figure 2) shows that this relationship is not well described by an exponential function. The measured data after longer hold times (e.g. t_4-t_8 in table 2) in particular, deviate from the expected exponential fit. This may be a function of counting statistics and/or the effects of thermal transfer, however this phenomena requires further investigation, currently beyond the scope of this paper. The Arrhenius plot constructed from elevated-temperature IR luminescence signals (figure 2) is associated with large uncertainties (typically 20-50%) and the relationship between Ln(τ) and temperature is not well approximated with a linear fit. Therefore, the E, s and τ_T values presented in table 3 based on the elevated temperature IR signals should be considered unreliable at present.

Table 3: Calculated E, s and τ_{20} for the same two aliquots of MAL05-01-01 (discs 1 and 2) measured using different LED wavelengths (λ), where 870 nm = IR, 525 nm = green and 470 nm = blue LEDs.

Disc	λ (nm)	E (eV)	s (s)	τ_{20} (a)

1	870	1.88 ± 0.16	$9.65*10^{15}$	$7.68*10^{8}$
	525	1.67 ± 0.08	$8.51*10^{13}$	$1.87*10^{7}$
	470	1.42 ± 0.13	$2.62*10^{12}$	$1.54*10^{6}$
2	870	1.99 ± 0.18	$1.38*10^{17}$	$3.72*10^{9}$
	525	1.52 ± 0.08	$6.37*10^{11}$	$1.42*10^{5}$
	470	1.41 ± 0.13	$4.25*10^{11}$	$1.17*10^{5}$

To test whether the discrepancies in E, s and τ_{20} by green/blue wavelength (table 3) are influenced by differing contributions of signal from the different OSL components, $E_{(t)}$, $s_{(t)}$ and $\tau_{20\ (t)}$ plots are presented in figure 3, alongside the % contribution of the fast, medium and slow components to the bulk signal at 0.1 s integrals. These data demonstrate that for both blue and green light stimulated signals, E, s and τ_{20} vary with the time integral used for calculation; falling as time is extended. Estimates for green-E values are consistent between 0.1 and 1 s (figure 3b), although there is a tendency for s to decrease during this period. In contrast, blue-E is lower than green-E, and also decreases with time (figure 3). s remains relatively stable within the first 0.2 s. With blue-light stimulation, the fast component contributes less than 50% of the signal in the first 0.1 s of stimulation, and it is suggested that the decrease in E and hence lifetime is due to the incorporation of signal from different traps (presumably the medium component, but perhaps the slow1 component identified by Jain et al. (2003) and Durcan and Duller (2011)). It is proposed that for this sample at least, signal contributions from non-fast component traps 'muddy' the calculated lifetime, particularly in the presence of a large contribution from the medium component (as is the case with this sample, e.g. figure 3a). This is observed particularly in the blue stimulated signals due to the wavelength dependencies of quartz photo-ionisation cross-sections (Singarayer and Bailey, 2004), where cross-section values for the fast and medium components converge with lower stimulation wavelengths. For samples where the fast component is dominant, lifetimes calculated from the initial part of the signal perhaps can be assumed to originate mostly from a single trap (e.g. the 325°C peak), which has been concluded in studies by Rhodes (1990) and Wintle and Murray (1998). However, for samples which have a significant contribution(s) from different component(s) in the initial part of the OSL signal, calculated lifetimes will reflect multiple-trap contributions of charge, as seen in these data (figure 3). If this is the case, the use of stimulation light with longer wavelengths is an option for better isolating signal from the fast component and the relatively lower de-trapping rates of the other components (in comparison to the fast) with longer stimulation wavelengths (c.f. Bailey et al., 2011).

3.2 Apparent lifetime variability induced during the isothermal decay protocol

As discussed, in the isothermal decay protocol τ_T is derived from the luminescence signal measured after a series of elevated temperature holds. To investigate the variability in measured E, s and τ_{20} that may be introduced by variations in the isothermal decay protocol, a jackknife approach was taken using the measured datasets. E, s and τ_{20} were re-calculated using i) different combinations of raised temperature hold times for τ_T calculation and ii) different temperature intervals for construction of the Arrhenius plot from which τ_T was calculated. This approach was applied to luminescence signals measured with blue and green light for both aliquots of sample, and an example of the induced variability for disc 1, measured with green light is shown in figure 2. This approach was not applied to elevated temperature IR signals, given the difficulties in deriving a lifetime, discussed in section 3.1.

The different symbols in figure 4 represent E, s and τ_{20} values derived from the same luminescence signals, but where τ_T has been calculated from different hold time combinations and temperature intervals. Individual E, s and τ_{20} values are normalised to values calculated where temperature interval is 5°C and holds $t_{1\text{-}8}$ are used. For the most part, E is consistently calculated to within ±5%, although E values are most

consistent when a shorter hold time (t_2 in table 2) is included immediately after the first elevated temperature hold (for 0s; t_1). Of the hold time combinations tested, the most consistent combinations for E calculation are t_{1-8}, t_{1-4} and t_{1-3} (figure 4). This suggests that the shorter hold times are relatively more important than the longer duration holds, presumably because they better constrain the exponential fit of the luminescence data for τ_T derivation in the area of the curve where the gradient is steepest (in absolute value). If the data could be fitted precisely (e.g. r^2=1) with an exponential function, the combination of hold times should not matter. However, uncertainties in the sensitised luminescence signals (L_x/T_x) lead to uncertainties in the mathematical fit, and focusing efforts on measuring luminescence signals after shorter, rather than longer, hold times should allow a better fitting of the relationship between luminescence signal and hold time, due to the lower uncertainties associated with counting statistics. For clarity, uncertainties associated with E are not plotted in figure 4, however are in the region of ~5%. Whilst the majority of E estimations are within uncertainties of each other, there is a tendency for lower E values as temperature interval is increased. The reason for the tendency for E to increase with greater number of empirically derived τ_T values is unknown. Presumably, more data leads to better fitting of the linear function in the Arrhenius plot, however that the gradient of this fit should consistently vary in one direction requires further exploration. That said, these data demonstrate that for the majority of elevated temperature hold combinations, E can be consistently determined (figure 4a). Greater confidence can be placed in determinations where emphasis is placed on shorter elevated temperature hold times for τ_T derivation and higher temperature intervals (ideally 5°C or 10°C).

When hold time combinations and temperature intervals are varied, greater variability is observed for estimates of s and therefore τ_T (figure 4). Again, the combination of focus on shorter elevated temperature hold times and narrower temperature intervals results in greater consistency between estimates. That s estimates display more variability is not surprising. s is derived through extrapolation from the empirical data to the ordinate on the Arrhenius plot. Therefore even small uncertainties in empirically derived τ_Ts results in the potential for greater variability approaching the ordinate. To minimise variability in s and τ_{20}, it is important that τ_T is calculated as precisely as possible. E and s are used to calculate τ_{20}, hence the trends in E and s variability are also seen in figure 4c. Focusing on elevated temperature hold time combinations which focus on the shorter times (e.g. t_{1-8}, t_{1-4} and t_{1-3}; table 2), lifetimes calculated from τ_{20} determinations from intervals of 20°C and 30°C appear to underestimate τ_{20} by up to 50% in comparison to the 5°C interval. For this sample at least, calculated signal lifetime estimates based on Arrhenius plots constructed using wider temperature intervals (>20°C) should be treated as minima.

3.3 τ_T uncertainty and the impact on lifetime calculation

To investigate the impact of uncertainty of τ_{20} estimates when temperature interval and τ_T uncertainty are varied, values for E and s were fixed and Arrhenius plots were simulated, producing 5,000 plots where the relationship between Ln(τ_T) and temperature was fit perfectly with a linear function. Uncertainties of ±1, ±5 and ±10% were applied to individual τ_T values, and τ_T temperature interval was varied between 2°C and 30°C (table 4). The trends observed in table 4 confirm those observed in the empirical data (figure 4). Trap depth is relatively insensitive to simulated temperature interval, and can be calculated consistently to within ±6% of the known value in the presence of τ_T uncertainties of up to ± 10% (table 4). Where individual uncertainties on τ_T do not exceed ±5%, in the majority of cases, E can be calculated to within ±3% of the fixed value. Simulated estimates of s, and therefore τ_{20}, are more variable, as is the case in the empirical evidence, with simulations producing positively skewed distributions for both parameters (e.g. table 4; figure 5). Relatively large, asymmetric uncertainties in s should be expected given the long extrapolation required in the Arrhenius plot to derive s. For example, simulations with τ_T uncertainties of ±5% and a

temperature interval of 20°C results in deviations from the fixed value of s and the calculated τ_{20} of ~-40% at the 5th percentile and >240% at the 95th percentile. To achieve an estimate of τ_{20} to within 10% of the target τ_{20} value (from fixed E and s), a temperature interval of 2°C and τ_T uncertainties of ±1% are required (table 4), which are both unlikely and impracticable in terms of measurement.

Table 4: Summary of data from simulated Arrhenius plots (n = 5000). Estimates of E, s and τ_{20} are normalised to the fixed values of E =1.65 eV, s = $1.25*10^{12}$ s^{-1} and therefore τ_{20} = $7.64*10^{8}$a, and the 5th, 50th and 95th percentiles are reported. Fixed E and s values were chosen to be representative of frequently reported averages (c.f. Preusser et al., 2009). Interval refers to the temperature interval used over the range of 240–300 °C, and uncertainty is the uncertainty attributed to individual τ_Ts. The ratio of estimated (est) to fixed values are shown.

	Interval	2°C			5°C			10°C			20°C			30°C		
	Uncertainty	±1%	±5%	±10%	±1%	±5%	±10%	±1%	±5%	±10%	±1%	±5%	±10%	±1%	±5%	±10%
	Percentile															
E_{est}/E_{fixed}	5th	1.00	0.99	0.97	1.00	0.98	0.96	1.00	0.98	0.95	0.99	0.97	0.94	0.99	0.97	0.94
	50th	1.00	1.00	1.00	1.00	1.00	1.00	1.00	1.00	1.00	1.00	1.00	1.00	1.00	1.00	1.00
	95th	1.00	1.01	1.03	1.00	1.02	1.04	1.00	1.02	1.05	1.01	1.03	1.06	1.01	1.03	1.06
s_{est}/ s_{fixed}	5th	0.92	0.64	0.41	0.87	0.52	0.27	0.84	0.43	0.17	0.82	0.37	0.13	0.81	0.35	0.12
	50th	1.00	1.01	1.01	1.00	1.00	1.00	1.00	1.01	1.01	1.00	1.01	1.00	1.00	1.00	1.02
	95th	1.09	1.58	2.54	1.14	1.95	3.95	1.19	2.34	5.22	1.22	2.78	7.34	1.23	2.96	8.69
$\tau_{20\_est}/ \tau_{20\_fixed}$	5th	0.95	0.70	0.48	0.91	0.59	0.33	0.88	0.50	0.23	0.86	0.44	0.18	0.85	0.42	0.16
	50th	1.02	1.03	1.03	1.02	1.02	1.01	1.02	1.03	1.03	1.02	1.03	1.01	1.02	1.03	1.05
	95th	1.10	1.50	2.24	1.15	1.80	3.26	1.18	2.11	4.12	1.22	2.43	5.46	1.22	2.56	6.19

4. Conclusion and Recommendations

This paper has sought to explore potential sources of variability which may arise through the use of the isothermal decay protocol and Arrhenius plots for lifetime determination of quartz OSL signals typically used in dating applications. Focus has been upon variations in the combination of elevated temperature hold times used for τ_T measurement, the number of τ_T points used to construct the Arrhenius plot, and the OSL stimulation wavelength. Using both empirical and modelled datasets, this paper has demonstrated that E can be calculated with relative consistency, in contrast to s, which is subject to more variability. This variability arises from the long extrapolation distance on the Arrhenius plot. Optimising combinations of hold times and temperature intervals used within the isothermal decay protocol can reduce variability, and this has been demonstrated with empirical and simulated data. The measurement of luminescence signals using various different wavelengths has shown that contributions from at least one non-fast OSL component can impact lifetime calculation. Stimulating luminescence with light of longer wavelengths (e.g. green light), and utilising the different wavelength dependencies of the fast and non-fast OSL components (Singarayer and Bailey, 2004), the signal from the fast OSL component can be better isolated from slower components. Reducing the contribution of non-fast component signal will allow more reliable estimates of lifetime.

On the basis of the presented datasets, the following recommendations are proposed for quartz OSL signal lifetime determination using isothermal decay:

i) Before estimates of the kinetic parameters of an OSL signal are made, the composition of the OSL under investigation should be assessed. Contributions of signal from multiple traps and/or poor mathematical fits to empirical data may render lifetime estimates inaccurate.

ii) In the presence of high signal contributions from non-fast OSL components, lifetimes may be affected by signal from more than one trap. These signal contributions can be minimised by stimulating luminescence with light of longer wavelengths to better isolate signal from the fast component from other quartz OSL signals.
iii) Lifetime calculations should be made for multiple aliquots of sample. Due to the nature of the mathematical fitting undertaken in the calculation of the lifetime, variability particularly in s should be expected. E can be calculated more reproducibility and can therefore be used to inform assessments of intra-sample variability.
iv) Improved reproducibility of lifetime estimates can be achieved by altering the isothermal decay protocol. Elevated temperature hold times should incorporate shorter times, where the gradient of the exponential fit is highest in absolute value. Temperature intervals of less than 10°C also provided improvements in reproducibility in this study.
v) Relatively large, asymmetric uncertainties are associated with estimates of s. Luminescence practitioners should bear this in mind, and report E, s and τ values with uncertainties.
vi) Simple modelling from fixed values of E and s can indicate the distribution of expected E and s values based on the protocol adopted for empirical data collection, and can be used to inform the precision of E, s and lifetime determinations.

Acknowledgements

The author thanks St John's College, Oxford for supporting attendance at the 15th Conference of Luminescence and Electron Spin Resonance Dating (LED2017), where this work was initially presented. Georgina King is thanked for commenting on an earlier version of this manuscript, as are Ann Wintle, Rachel Smedley, Richard Bailey and Sally Lowick for their thoughts and discussion. Comments and suggestions from two anonymous reviewers significantly improved this manuscript.

References

Aitken, M.J., 1985. Thermoluminescence dating. Academic Press, London.

Ankjægaard, C., Jain, M. and Wallinga, J., 2013. Towards dating Quaternary sediments using the quartz Violet Stimulated Luminescence (VSL) signal. Quaternary Geochronology, 18, 99-109.

Bailey, R.M., 1998a. The form of the optically stimulated luminescence signal of quartz: implications for dating. Unpublished Ph.D. thesis, University of London.

Bailey, R.M., 1998b. Depletion of the quartz OSL signal using low photon energy stimulation. Ancient TL, 16, 33-36.

Bailey, R.M., 2010. Direct measurement of the fast component of quartz optically stimulated luminescence and implications for the accuracy of optical dating. Quaternary Geochronology, 5, 559-568.

Bailey, R.M., Yukihara, E.G. and McKeever, S.W.S., 2011. Separation of quartz optically stimulated luminescence components using green (525 nm) stimulation. Radiation Measurements, 46, 643-648.

Buechi, M.W., Lowick, S.E. and Anselmetti, F.S., 2017. Luminescence dating of glaciolacustrine silt in overdeepened basin fills beyond the last interglacial. Quaternary Geochronology, 37, 55-67.

Bulur, E., 2000. A simple transformation for converting CW-OSL curves to LM-OSL curves. Radiation Measurements, 32, 141-145.

Duller, G.A.T., Penkman, K.E.H. and Wintle, A.G., 2009. Assessing the potential for using biogenic calcites as dosimeters for luminescence dating. Radiation Measurements, 44, 429-433.

Durcan, J.A. and Duller, G.A.T., 2011.The fast ratio: a rapid measure for testing the dominance of the fast component in the initial OSL signal from quartz. Radiation Measurements, 46, 1065-1072.

Fan, A., Li, S.-H. and Li, B., 2009. Characteristics of quartz infrared stimulated luminescence (IRSL) at elevated temperatures. Radiation Measurements, 44, 434-438.
King, G.E., Guralnik, B., Valla, P.G. and Herman, F., 2016. Trapped-charge thermochronometry and thermometry: a status review. Chemical Geology, 446, 3-17.
Jain, M., Murray A.S. and Bøtter-Jensen, L., 2003. Characterisation of blue-light stimulated luminescence components in different quartz samples: implications for dose measurement. Radiation Measurements, 37, 441-449.
Jain, M., Murray, A.S., Bøtter-Jensen, L. and Wintle, A.G., 2005. A single-aliquot regenerative-dose method based on IR (1.49 eV) bleaching of the fast OSL component in quartz. Radiation Measurements, 39, 309-318.
Li, S.-H. and Chen, G., 2001. Studies of thermal stability of trapped charges associated with OSL from quartz. Journal of Physics D: Applied Physics, 493-498.
Li, S.-H. and Tso, M.-Y. W., 1997. Lifetime determination of OSL signals from potassium feldspars. Radiation Measurements, 27, 119-121.
Lowick, S.E. and Valla, P.G., 2018. Characterising the luminescence behaviour of 'infinitely old' quartz samples from Switzerland. Quaternary Geochronology, 43, 1-11.
McKeever, S.W.S., 1985. Thermoluminescence of solids. Cambridge University Press, Cambridge.
Murray, A.S. and Wintle, A.G., 1999. Isothermal decay of optically stimulated luminescence in quartz. Radiation Measurements, 30, 119-125.
Preusser, F., Chithambo, M.L., Gotte, T., Martini, M., Ramseyer, K., Sendezera, E.J., Susino, G.J. and Wintle, A.G., 2009. Quartz as a natural luminescence dosimeter. Earth Science Reviews, 97, 184-214.
Rhodes, E.J., 1988. Methodological considerations in the optical dating of quartz. Quaternary Science Reviews, 7, 395-400.
Schmidt, C., Friedrich, J., Adamiec, G., Chruścińska, A., Fasoli, M., Kreutzer, S., Martini, M., Panzeri, L., Polymeris, G.S., Przegietka, K., Valla, P.G., King, G.E., and Sanderson, D.C.W., 2018. How reproducible are kinetic parameter constraints of quartz luminescence? An interlaboratory comparison for the 110 °C TL peak. Radiation Measurements, 110, 14-24.
Singarayer, J.S. and Bailey, R.M., 2004. Component- resolved bleaching spectra of quartz optically stimulated luminescence: preliminary results and implications for dating. Radiation Measurements, 38, 111-118.

Spooner, N.A. and Questiaux, D.G., 2000. Kinetics of red, blue and UV thermoluminescence and optically stimulated luminescence from quartz. Radiation Measurements, 32, 659-666.
Thomas, D.S.G., Bailey, R.M., Shaw, P.A., Durcan, J.A., Singarayer, J.S., 2009. Late Quaternary highstands at Lake Chilwa, Malawi: Frequency, timing and possible forcing mechanisms in the last 44ka. Quaternary Science Reviews, 28, 526-539.
Thomsen, K.J., Murray, A.S., Jain, M. and Botter-Jensen, L., 2008. Laboratory fading rates of various luminescence signals from feldspar-rich sediment extracts. Radiation Measurements, 43, 1474-1486.
Trauerstein, M., Lowick, S.E., Preusser, F. and Veit, H., 2017. Testing the suitability of dim sedimentary quartz from northern Switzerland for OSL burial dose estimation. Geochronometria, 44, 66-76.
Wang, X.L., Wintle, A.G. and Lu, Y.C., 2006. Thermally transferred luminescence in fine-grained quartz from Chinese loess: Basic observations. Radiation Measurements, 6, 649-658.
Wintle, A.G. and Murray, A.S., 1998. Towards the development of a preheat procedure for OSL dating of quartz. Radiation Measurements, 29, 81-94.

Figure Captions

Figure 1: Left, sensitivity corrected green stimulated luminescence recorded after various storage times at temperatures 240, 250, 260, 270, 280, 290, and 300°C (for disc 1), and the Arrhenius plot constructed from these data (middle). Right, the relationship between hold time and luminescence at a hold time of 240°C, when disc 1 was stimulated with blue, green and IR light. Inset, the Arrhenius plot constructed from the luminescence data stimulated with different wavelengths.

Figure 2: Sensitivity corrected luminescence recorded after various storage times at temperatures 240°C, 270°C and 300°C, used to calculate τT (disc 1). Luminescence was stimulated using infra-red light at 160°C (e.g. table 1b). The exponential fits to the data are shown. Note, the first elevated temperature holds were for 0 s, but are plotted at 0.01 s for display purposes. Inset, the Arrhenius plot constructed from elevated temperature IR stimulated luminescence signals (disc 1).

Figure 3: E, s and τ20 by time integrals of 0.1 s using blue-stimulated (a) and green stimulated (b) luminescence signals (disc 1). Also shown, the % contribution of fast, medium and slow component signal per time integral, obtained by curve fitting of continuous-wave OSL signals.

Figure 4: Variability in E, s, and τ20 as elevated temperature hold time and temperature interval are varied (green stimulated luminescence signals from disc 1). In all iterations, the temperature range is 240-300°C, where an interval of 5°C means τT was calculated at 240, 245, 250 … 300°C etc.. Different hold time combinations are indicated by the different symbols. Values are normalised to the value calculated from a temperature interval of 5°C and hold time combinations t1-8.

Figure 5: Distributions of E, s and τ20 calculated from 5,000 simulated Arrhenius plots, using fixed values of E and s (E = 1.65 eV, s = 1.25*1012s, and therefore τ20 = 7.64*108 a, shown by the vertical reference lines. An uncertainty of ±5% is ascribed to τT values, and the temperature interval used and 20°C.

Figure 1

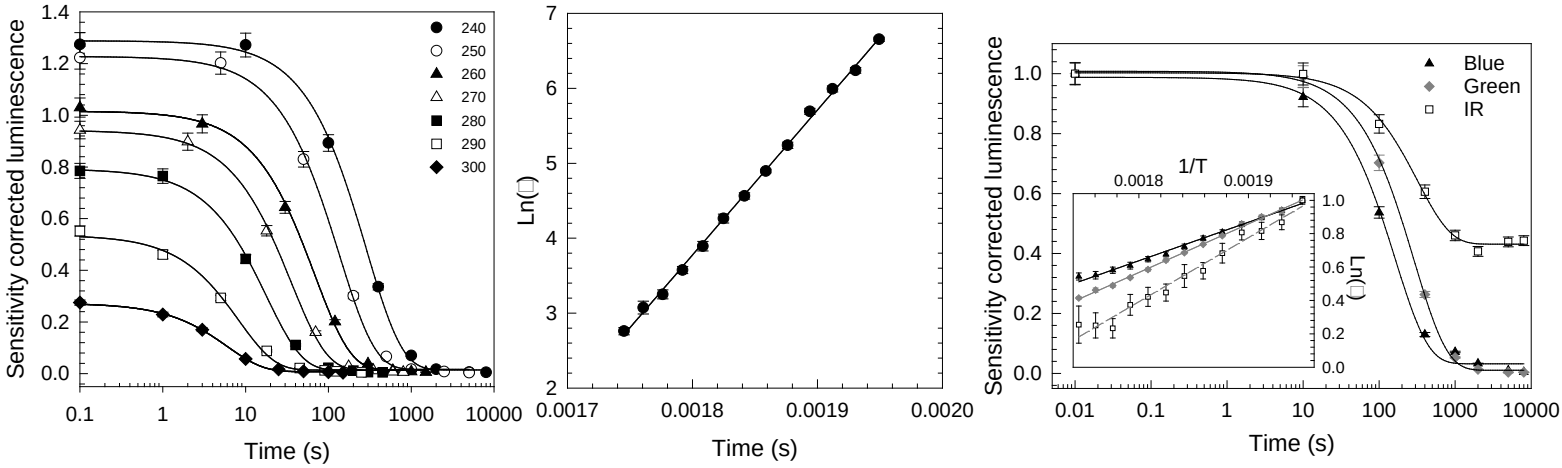

Figure 2

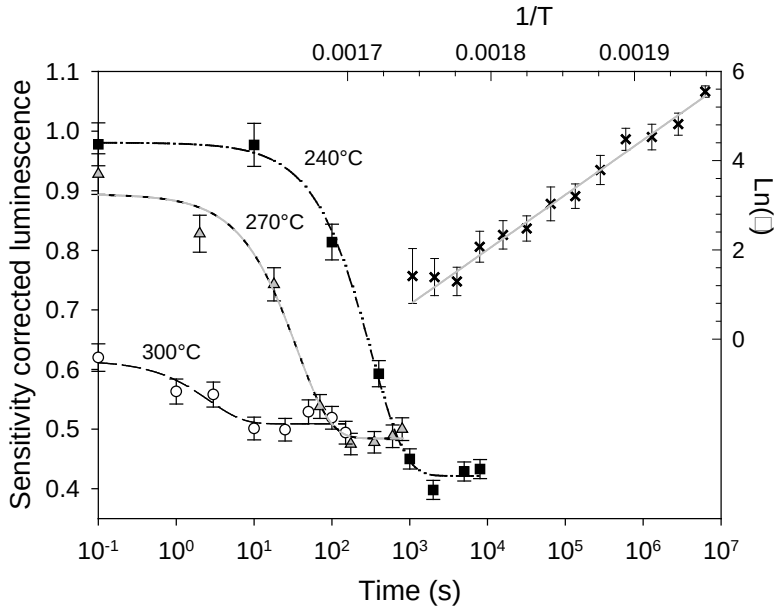

Figure 3

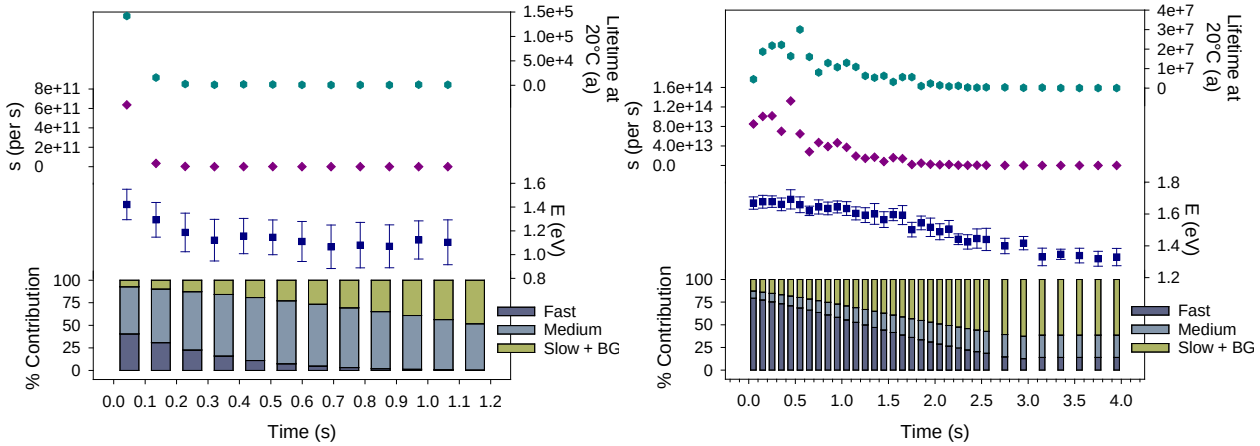

Figure 4

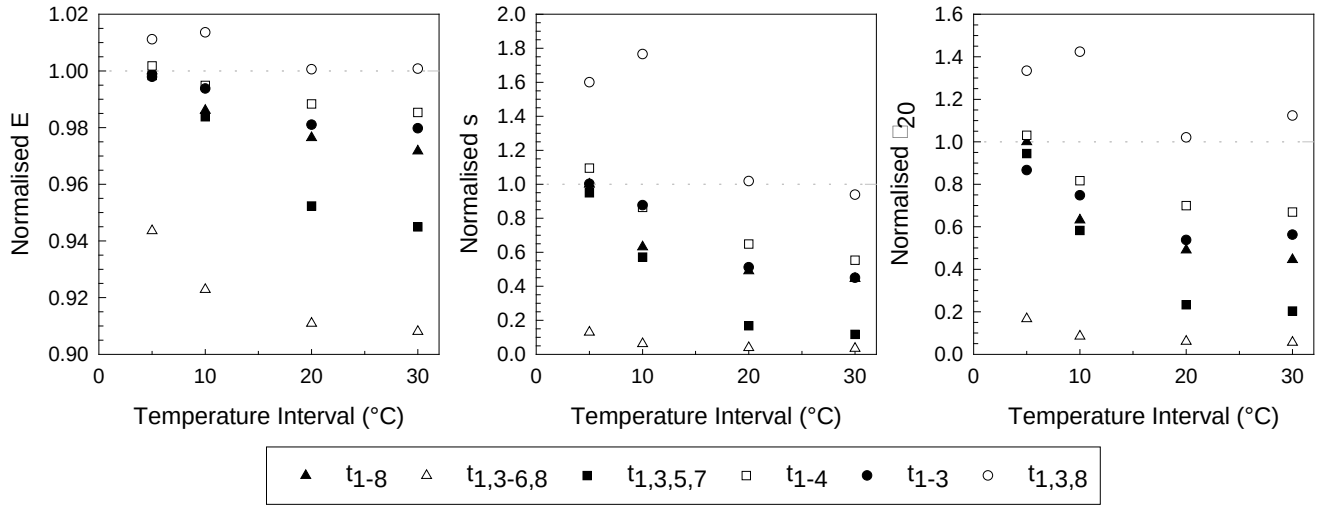

Figure 5